Current Research (2023) Newfoundland and Labrador Department of Industry, Energy and Technology
Geological Survey, Report 23-1, pages 31-46

GABBRO INTRUSIONS ALONG THE DOG BAY LINE–APPLETON FAULT ZONE GOLD CORRIDOR, NORTHEAST–CENTRAL NEWFOUNDLAND: U–Pb BADDELEYITE GEOCHRONOLOGY AND LITHOGEOCHEMISTRY

I.W. Honsberger, H.A.I. Sandeman[1], W. Bleeker and S.L. Kamo[2]
Natural Resources Canada, Geological Survey of Canada, 601 Booth Street, Ottawa, ON, K1A 0E8
[1]Mineral Deposits Section
[2]Jack Satterly Geochronology Laboratory, Department of Earth Sciences, University of Toronto, 22 Ursula Franklin Street, Toronto, ON, M5S 3B1

ABSTRACT

The Dog Bay Line–Appleton Fault Zone gold corridor in the Exploits Subzone of northeast–central Newfoundland is prospective for orogenic gold mineralization; however, the history of deposition, magmatism, faulting, and tectonism is not fully constrained. Gold-bearing, gabbroic hypabyssal intrusions (dykes and sills), within the clastic sedimentary rocks of the Davidsville Group, Indian Islands Group and Ten Mile Lake Formation, provide insight into the timing of magmatism and tectonic evolution along the structural corridor.

This contribution presents a new, Late Ordovician (Katian), high-precision U–Pb minimum baddeleyite age of 446.30 ± 0.44 Ma for an auriferous gabbro intrusion, the Midway Gabbro, from Labrador Gold Corporation's Kingsway gold project. This Katian age provides a maximum age constraint on post-intrusion orogenic gold mineralization.

The hypabyssal gabbro intrusions along the Dog Bay Line–Appleton Fault Zone gold corridor are grouped broadly into two lithogeochemical types. Type 1 gabbros are tholeiitic back-arc basin melts with minor light rare-earth and large-ion lithophile element enrichments, and variably developed high-field-strength-element troughs. Type 2 gabbros are transitional to calc-alkaline, arc-like magmas having modest to significant enrichment in light-rare-earth elements and large-ion lithophile elements. Both Type 1 and Type 2 gabbros were emplaced in the Late Ordovician, whereas Silurian–Devonian gabbros are Type 2 only. Late Ordovician Type 1 and Type 2 gabbros may have formed in the Tetagouche–Exploits back-arc basin.

These findings indicate that gabbro intrusions along the Dog Bay Line–Appleton Fault Zone gold corridor record a Late Ordovician to Devonian, polyphase, tectonomagmatic history from an intra-oceanic arc to an intracontinental deformation zone associated with orogenic gold mineralization. Imbrication of sedimentary–magmatic rock sequences along the gold corridor is attributed to Devonian deformation during the Acadian orogenic cycle, likely followed by Neo-Acadian (Late Devonian) and Carboniferous transpressive–transtensional along-strike displacement and dismemberment of the Acadian orogenic collage.

INTRODUCTION

The present-day "gold rush" on the Island of Newfoundland is focused along fault zones that crosscut sedimentary–magmatic terranes of the Exploits Subzone and Gander Zone (Figure 1; Williams *et al.*, 1988). Two major structural corridors in the Exploits Subzone are undergoing intense exploration for orogenic gold mineralization. One corridor extends for ~300 km northeast between Cape Ray on the southwestern coast and Mount Peyton in central Newfoundland (Figure 1). This corridor includes Marathon Gold Corporation's ~5 Moz Valentine Lake gold deposits, as well as the Cape Ray, Wood Lake, Wilding Lake and Moosehead gold prospects (Figure 1; Tuach *et al.*, 1988; Colman-Sadd *et al.*, 1990; Evans, 1996; Valverde-Vaquero *et al.*, 2006; Honsberger *et al.*, 2022a). In northeast–central Newfoundland, the other prospective structural corridor trends north-northeast for at least 75 km along the Dog Bay Line and Appleton Fault Zone near Glenwood–Appleton (Figure 2). New Found Gold Corporation's bonanza-style Keats and Lotto zones, part of their Queensway gold project (Srivastava, 2022), occur adjacent to and immediately southeast of the Appleton Fault Zone, whereas Labrador Gold Corporation's Big Vein discovery, part of their Kingsway gold project (Moss, 2022), is immediately northwest of the Appleton Fault Zone (Figure

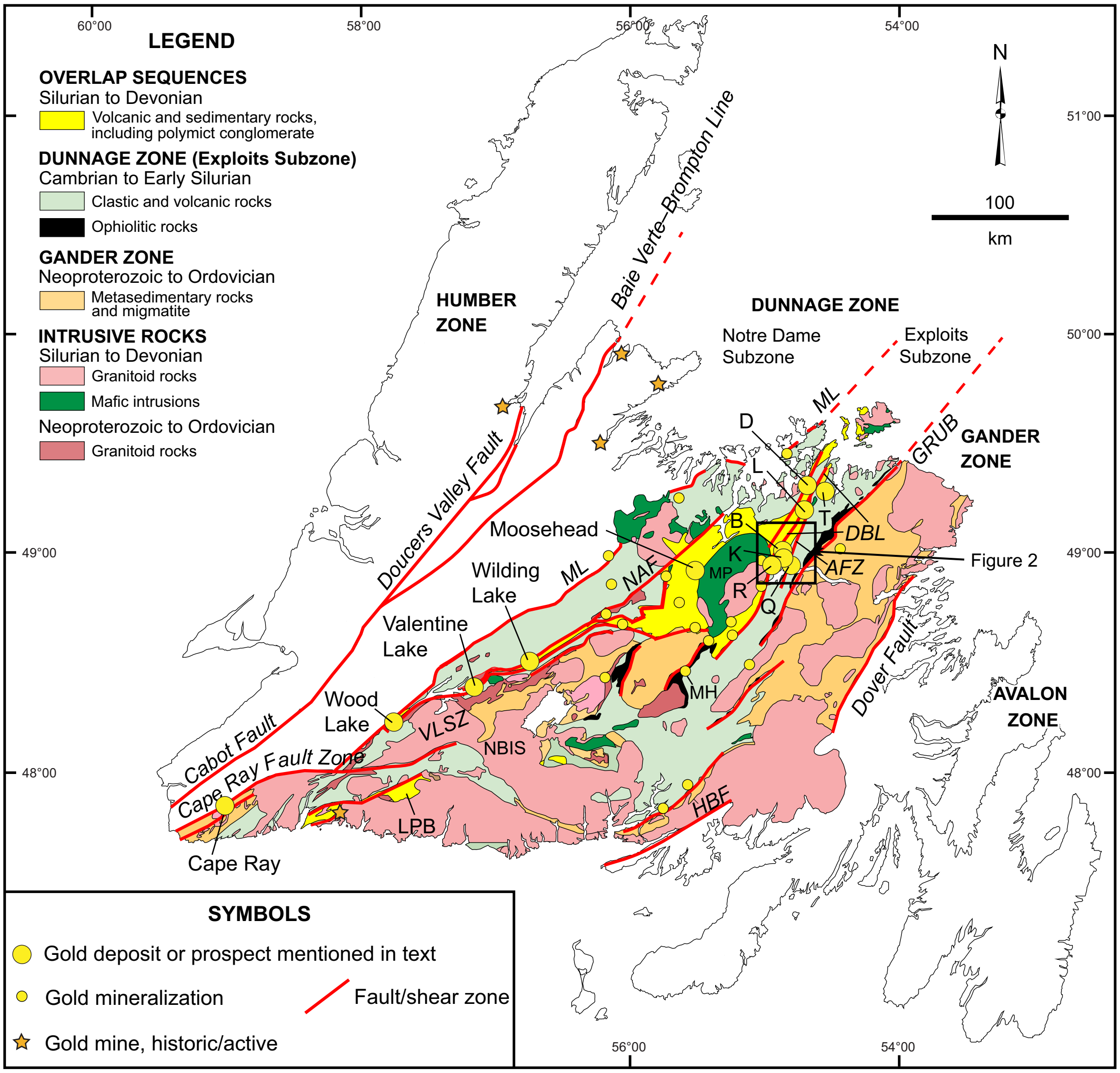

Figure 1. *Generalized geological map of the Exploits Subzone and Gander Zone of central Newfoundland, with selected gold occurrences shown (gold occurrences are from the Geological Survey of Newfoundland and Labrador, Department of Industry, Energy and Technology's Mineral Occurrence Database). Map modified from Colman-Sadd* et al. *(1990). Fault zone names are in italics. Abbreviations: AFZ–Appleton Fault Zone; B–Big Pond gabbro; DBL–Dog Bay Line; D–Duder Lake (Corvette and Goldstash gabbros); GRUB–Gander River Complex Fault Zone; HBF–Hermitage Bay Fault; K–Kingsway gold project; L–Lucky Moose gabbro; LPB–La Poile Basin; MH–Mosquito Hill gold prospect; ML–Mekwe'jit Line; MP–Mount Peyton Intrusive Suite; NAF–Northern Arm Fault; NBIS–North Bay Intrusive Suite; Q–Queensway gold project; R–Road Breccia gabbro; T–Titan gabbro; VLSZ–Victoria Lake Shear Zone.*

Figure 2. *Simplified geological map and cross section of the northeastern Dunnage Zone and the setting of gabbro intrusions and gold mineralization along the Dog Bay Line–Appleton Fault Zone gold corridor. The map is based on https://geoatlas.gov.nl.ca/Default.htm, O'Brien (2003) and new observations. Sample localities include, from north to south: Big Pond gabbro (gold showing west of Big Pond), Cracker gabbro, Midway Gabbro (446 ± 0.4 Ma,* this study*), gabbro ~1 km west of Big Vein (no symbol), and Road Breccia gabbro (411 ± 5 Ma, McNicoll* et al*., 2006). The Midway Gabbro is projected onto the plane of the cross section. The Mount Peyton monzogranite ages are from Sandeman* et al. *(2017) (418 ± 1.6 Ma) and Dickson* et al. *(2007) (411 ± 3 Ma). Abbreviations: AFZ–Appleton Fault Zone; BV–Big Vein; DBL–Dog Bay Line; DG–Davidsville Group; IIG–Indian Islands Group; K–Keats Zone; GRC–Gander River Complex; JBP–Joe Batts Pond Fault Zone; MPIS–Mount Peyton Intrusive Suite; TML–Ten Mile Lake Formation.*

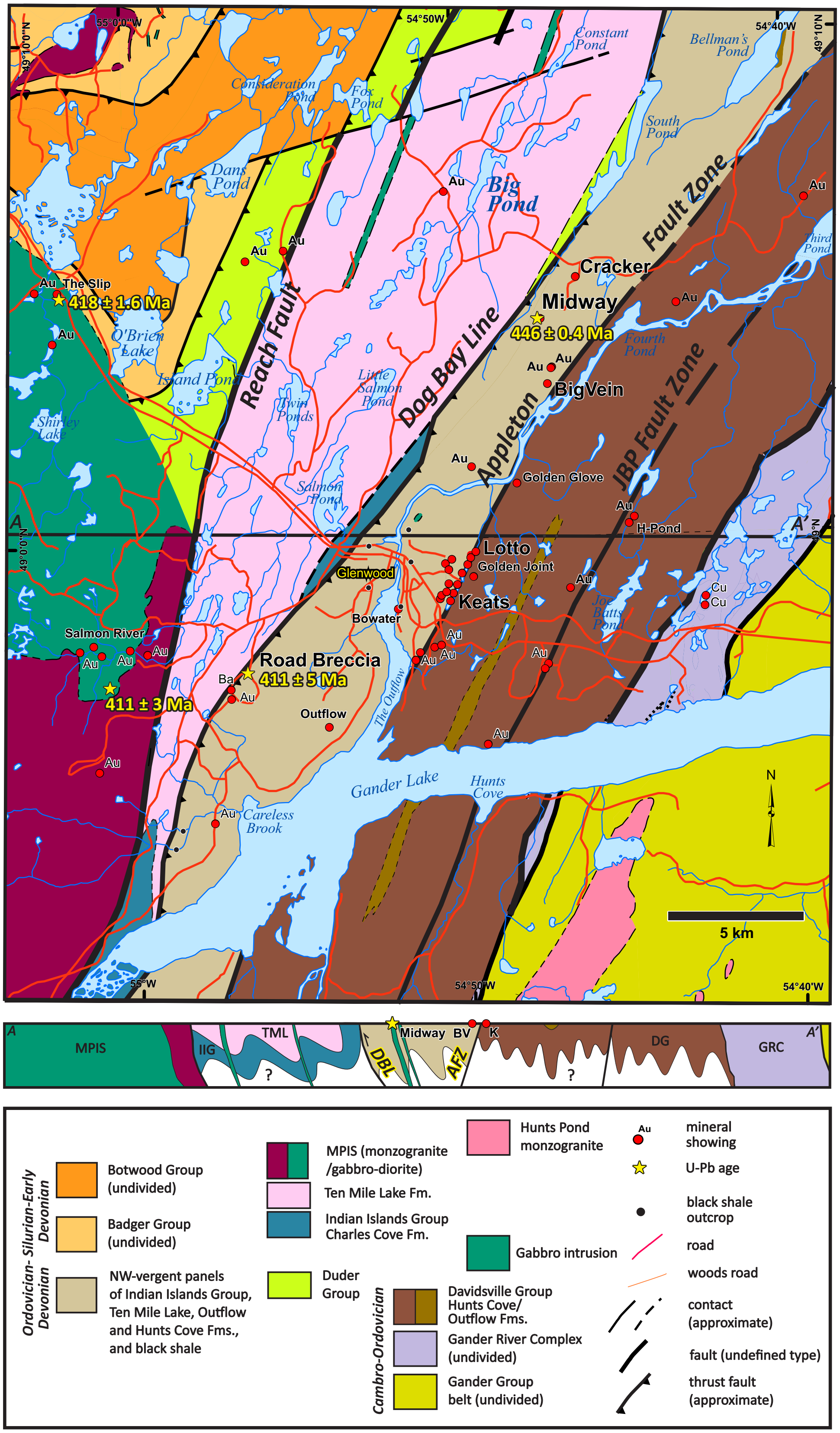

Figure 2. *Caption on previous page.*

2). Gold exploration, leading to mine development along the Victoria Lake–Valentine Lake belt, has been advancing since the discovery of the Valentine Lake mineralization in 1986 (Tuach *et al.*, 1988; Evans, 1996; Sandeman *et al.*, 2022). Exploration is in much earlier stages along the Dog Bay Line–Appleton Fault Zone gold corridor in northeast–central Newfoundland. Therefore, the setting, controls, and geological history of orogenic gold mineralization are relatively well constrained near Valentine Lake (*e.g.*, Lincoln *et al.*, 2018; Honsberger *et al.*, 2022a) compared to those in the northeast.

This contribution presents research on the age and lithogeochemistry of gabbro intrusions along the Dog Bay Line–Appleton Fault Zone gold corridor in northeast–central Newfoundland (Figure 2). A high-precision Late Ordovician (Katian; 446.30 ± 0.44 Ma) isotope dilution-thermal ionization mass spectrometry (ID-TIMS) U–Pb baddeleyite age is presented for the gold-bearing Midway Gabbro on Labrador Gold Corporation's Kingsway gold project. The Midway Gabbro is one intrusion within a more regionally extensive (~1400 km^2) northeast-trending zone of gold-mineralized gabbro showings along the Dog Bay Line and Appleton Fault Zone (Churchill and Evans, 1992; Evans and Hayes, 1992; Churchill *et al.*, 1993; Churchill, 1994; Currie, 1995a, b; Squires, 2005; Dickson *et al.*, 2007; McNicoll *et al.*, 2006; Moss, 2022). This study improves the understanding of the timing and tectonic setting of mafic magmatism associated with gold-mineralized structures in northeast–central Newfoundland.

REGIONAL GEOLOGY

The Dog Bay Line and Appleton Fault Zone are the two main deformation zones associated with orogenic gold mineralization in the Exploits Subzone of northeast–central Newfoundland (Figure 2; Evans, 1996; Sandeman *et al.*, 2022). The Dog Bay Line is described as a high-strain zone, consisting of a tectonic mélange that separates continental shelf and basinal sedimentary rocks of the Ganderian leading edge from the remnant fragments of Iapetus attached to the Notre Dame arc and trailing edge of Dashwoods terrane (Piasecki, 1992; Currie, 1993; Williams, 1993; Williams *et al.*, 1993; Pollock *et al.*, 2007). To the southeast of the Dog Bay Line are the turbiditic Davidsville Group, black shale of the Sandbian–Katian Main Point Formation, and their inferred Silurian cover sequence, the Indian Islands Group. To the northwest of the Dog Bay Line, are the oceanic rocks of the Exploits and Duder groups, black Sandbian–Katian shale of the Lawrence Harbour Formation (and equivalents), and the trench-fill, turbiditic Badger Group, all overlain by the volcanic and siliciclastic cover sequences of the Botwood Group (Dickson *et al.*, 2000; O'Brien, 2003; Dickson *et al.*, 2006). The siliciclastic, dominantly reddish sandstone sequence of the Ten Mile Lake Formation is inferred to stratigraphically overlie all units and the Dog Bay Line (Williams *et al.*, 1993; Currie, 1995a).

The Dog Bay Line is considered by some workers to represent the terminal, overall northwest-dipping (present-day coordinates) Salinic suture separating lower plate, peri-Gondwanan rocks of the Davidsville and Indian Islands groups from upper plate, peri-Laurentian rocks of the Badger and Botwood groups (Williams, 1993; Williams *et al.*, 1993; Currie, 1995a; Pollock *et al.*, 2007; Reusch and van Staal, 2012). Others argue that the Dog Bay Line is an overall southeast-dipping deformation zone that imbricated Ordovician to Early Devonian clastic sedimentary rock slices during Acadian intracontinental deformation (Figure 2; Dickson, 2006; Honsberger *et al.*, 2022b; H.A.I. Sandeman and I.W. Honsberger, unpublished data, 2023). The Appleton Fault Zone (Figure 2) is a corridor of strong deformation within the shale and turbidites of the Davidsville Group, unexposed at the surface. This blind fault, intersected during drilling at the Keats Zone, is interpreted as the major structural control on quartz vein-hosted gold mineralization on New Found Gold Corporation's Queensway project and Big Vein on Labrador Gold Corporation's Kingsway project (Moss, 2022; Srivastava, 2022).

Along the Dog Bay Line–Appleton Fault Zone gold corridor, the Davidsville Group consists of the turbidite-dominated Outflow Formation (Plate 1) and the shale-dominated Hunts Cove Formation, whereas calcareous sandstone–siltstone and sparse limestone of the Charles Cove and Seal Island formations, respectively, comprise the Indian Islands Group (Currie, 1995a; Dickson, 2006; Dickson *et al.*, 2007). These sedimentary rocks are moderately to strongly deformed and altered, particularly near fault zones, where they are isoclinally folded and characterized by a steeply dipping to vertical, slaty, bedding-parallel

Plate 1. *Field and drillcore photographs by I.W. Honsberger. A) Outflow Formation turbidite near Midway Gabbro. Note the thick sandstone (ss) beds and thin shale (shl) beds. NRCan photo 2022-578; B) Ten Mile Lake Formation grey-black shale, with quartz veins, cut by Big Vein. NRCan photo 2022-579; C) Iron carbonate alteration, quartz veins, and arsenopyrite (apy) and pyrite (py) in gold-bearing Midway Gabbro drillcore. NRCan photo 2022-580; D) Close-up of drillcore in C) showing coarse-grained arsenopyrite (apy). NRCan photo 2022-581; E) Gabbro intrusion (Cracker gabbro), with quartz vein, cutting black shale. NRCan photo 2022-582; F) Gabbro intrusion cutting shale, adjacent and to the west of the Dog Bay Line on Labrador Gold's Kingsway gold project. NRCan photo 2022-583.*

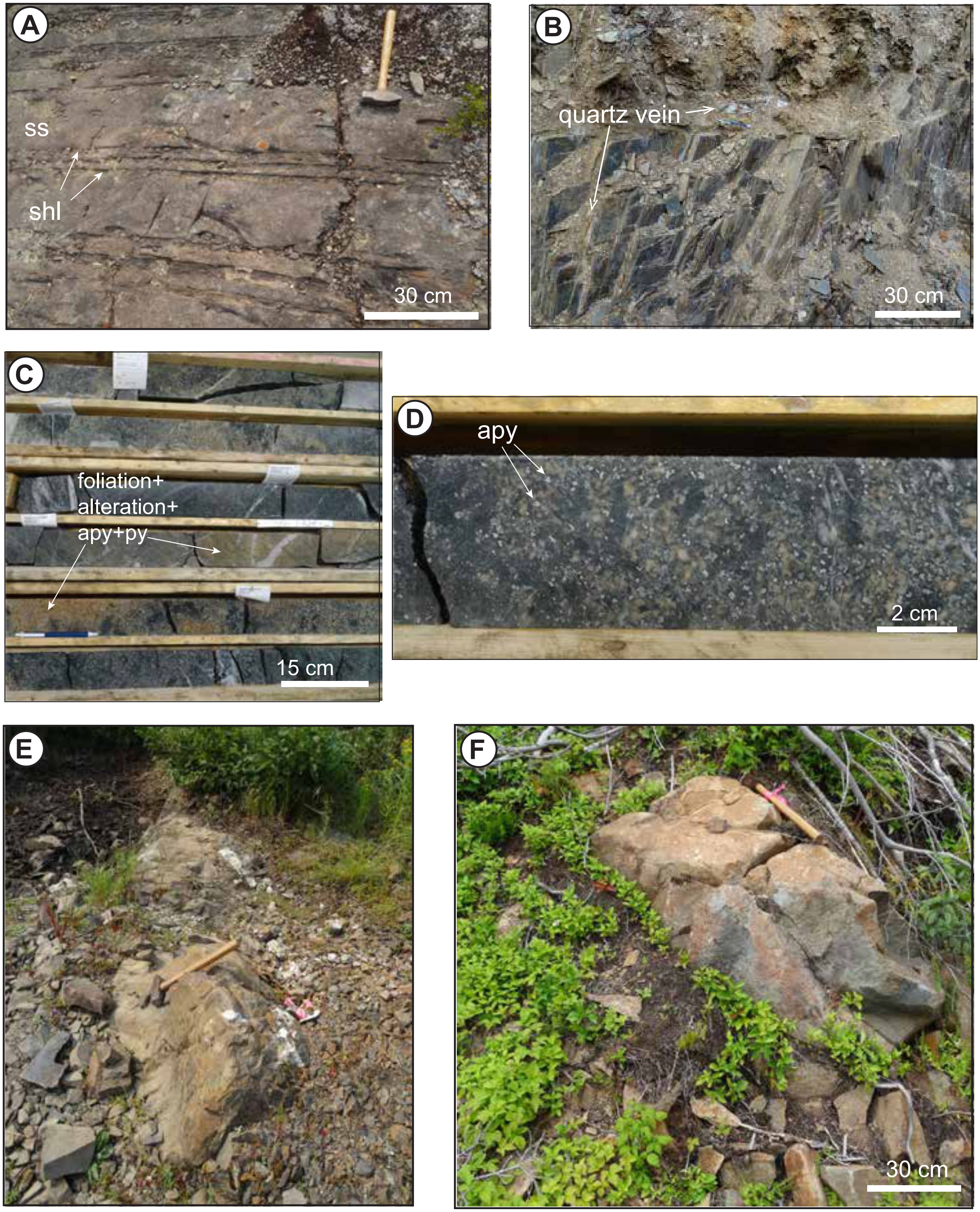

Plate 1. *Caption on previous page.*

cleavage (Figure 2, cross-section and Plate 1B; H.A.I. Sandeman and I.W. Honsberger, unpublished data, 2023.).

Between Gander Lake and the northern coastline of Newfoundland, numerous gabbro dykes and/or sills intrude sedimentary rocks of the Davidsville Group, Indian Islands Group, and Ten Mile Lake Formation (Figure 2 and Plate 1C–F; Churchill and Evans, 1992; Evans and Hayes, 1992; Churchill *et al.*, 1993; Currie, 1995a; Squires, 2005; McNicoll *et al.*, 2006; Dickson *et al.*, 2007). The southwestern end of this zone of gabbro occurrences, as currently defined, is adjacent to and to the east of the *ca.* 424–418 Ma bimodal Mount Peyton Intrusive Suite (Figure 2; Strong, 1979; Squires, 2005; Dickson *et al.*, 2007; Sandeman *et al.*, 2017). There, the epizonal, vuggy quartz-bearing Road Breccia gold showing is hosted in a *ca.* 411 Ma gabbro intrusion that cuts sandstone–siltstone of the Charles Cove Formation, Indian Islands Group (Figure 2; McNicoll *et al.*, 2006).

Many of the gabbro intrusions along the Dog Bay Line–Appleton Fault Zone gold corridor are cut by networks of quartz veins and shear zones that are prospective for orogenic gold mineralization (Churchill *et al.*, 1993; Evans, 1996; Squires, 2005). In the northeast, ~6 km to the east of Duder Lake, the Titan gabbro (Figure 1) intrudes the Silurian Indian Islands Group (McNicoll *et al.*, 2006) and hosts an orogenic gold prospect, currently being drilled by Exploits Discovery Corporation, following up on high-grade gold recognized during earlier drilling (Crosshair Exploration and Mining Corporation, press release, September 9, 2004). The Titan gabbro yielded a SHRIMP U–Pb zircon date of 381 ± 5 Ma; interpreted as a maximum igneous crystallization age for the quartz-veined, altered and gold-bearing host rock (McNicoll *et al.*, 2006). The gabbros at Duder Lake host structurally controlled gold mineralization at the Goldstash and Corvette prospects (Churchill and Evans, 1992; Churchill *et al.*, 1993; Churchill, 1994). The leucoxene-altered (titanite–ilmenite–rutile) gabbro intrusion that hosts the Corvette gold prospect yields a SHRIMP U–Pb baddeleyite age of 453 ± 1.3 Ma (Dickson *et al.*, 2007). Other gabbro intrusions along the Dog Bay Line–Appleton Fault Zone gold corridor that are prospective for gold mineralization include those of the Mount Peyton Intrusive Suite (Sandeman *et al.*, 2017) and those that occur north of the Gander River near Big Pond (Figure 2; Evans, 1996; Squires, 2005).

GABBRO SAMPLES

Regional field studies were carried out within the Davidsville Group, Indian Islands Group and Ten Mile Lake Formation along the Dog Bay Line–Appleton Fault Zone gold corridor (Figure 2). Eleven gabbro intrusions were sampled for lithogeochemistry (16 samples), with one gabbro sample (Midway Gabbro) analyzed for U–Pb geochronology. The samples include five from Labrador Gold Corporation's Kingsway gold project, three from the Road Breccia gabbro showing, two each from the Titan, Goldstash, and Corvette gabbro gold showings, and one each from the Big Pond and Lucky Moose gabbro gold showings to the northwest and northeast, respectively, of the Kingsway gold project (Figures 1 and 2). The gabbro intrusions from the Kingsway project (Moss, 2022) include the Cracker gabbro and Midway Gabbro, both hosts to gold showings, a gabbro ~1 km west of Big Vein, and two gabbro intrusions to the north-northwest of the Midway Gabbro (Figure 2 and Plate 1C–E).

The gabbro that occurs ~1 km west of the gold-mineralized Big Vein is a medium-grained, moderately deformed and altered intrusion cut by a 10- to 15-cm-wide lamprophyre dyke; no other contacts are exposed. The Cracker gabbro is a 0.5- to 1-m-wide gold-mineralized dyke that cuts deformed black shale (Figure 2 and Plate 1E). The dyke is fine to medium grained, massive, very weakly altered, and is locally cut by a thin (~10-cm-wide) quartz vein. The Midway Gabbro occurs ~1 km southwest of the Cracker gabbro. The Midway Gabbro is strongly weathered to brown and white, medium to coarse grained, massive to moderately deformed, and ranges from unaltered to strongly altered (Plates 1C–D and 2). In 2022, diamond drilling of the Midway Gabbro yielded up to 1.72 g/t gold over 17 m of drillcore, with higher grade zones of up to ~5 and 6 g/t gold over 3 to 4 m of drillcore (Moss, 2022). Based on drilling and geophysical data, the Midway Gabbro is interpreted to trend northeast for ~1 km and dip steeply to the east, but its thickness is not well constrained (Moss, 2022). The ID-TIMS U–Pb baddeleyite geochronology was applied to a sample of the Midway Gabbro collected from the only known surface exposure, an ~4 m^2 isolated outcrop surrounded by bog and glacial till.

Follow-up mineralogical analyses of the Cracker gabbro, Midway Gabbro, and the gabbro ~1 km west of Big Vein show that these samples are very similar with respect to their primary and secondary mineral assemblages, with the proportion of secondary minerals reflecting the intensity of alteration. The primary mineral assemblages are dominated by plagioclase laths and subhedral amphibole grains (Plate 2). Disseminated primary sulphide mineral assemblages include pyrite, chalcopyrite, sphalerite, and minor arsenopyrite (Plate 2). Secondary alteration minerals include arsenopyrite, siderite, calcite, chlorite, muscovite, leucoxene, potassium feldspar and epidote (Plate 2). The Midway Gabbro is particularly rich in arsenopyrite (Plate 1C–D). Zones of strong alteration in the Midway Gabbro contain abundant siderite, leucoxene, and sericite (Plate 2). Chlorite

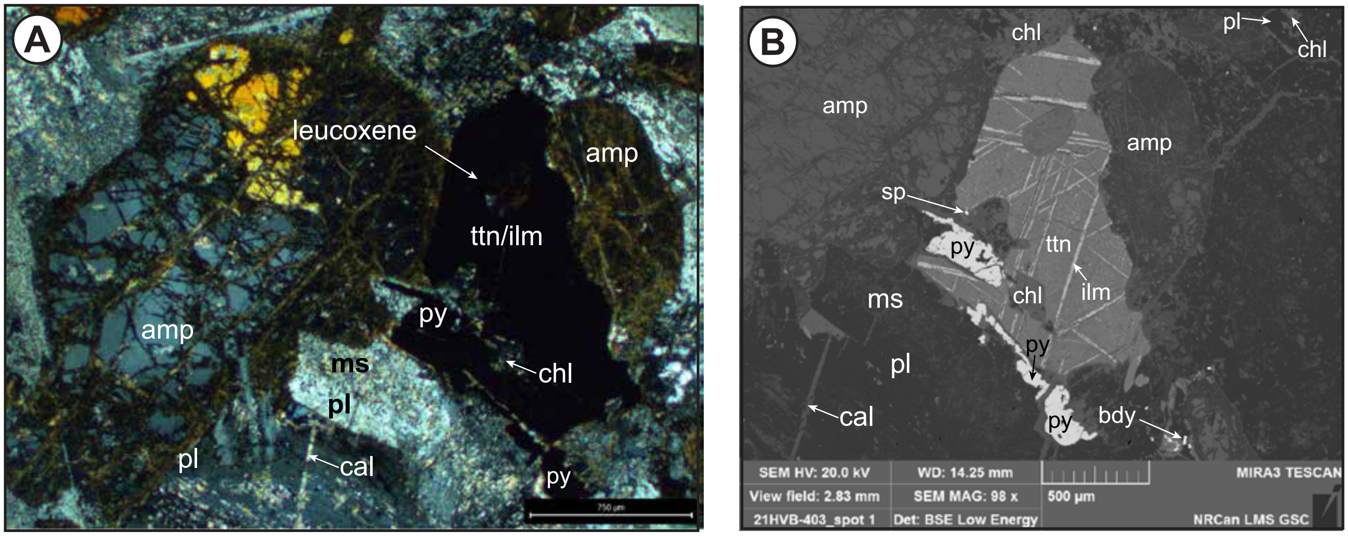

Plate 2. *Midway Gabbro mineral textures. A) Microphotograph (cross-polarized light) of Midway Gabbro showing a matrix of amphibole (amp) and plagioclase (pl) altered to muscovite (ms)-, chlorite (chl)-, calcite (cal)- and leucoxene. Opaque grain is titanite (ttn) with ilmenite (ilm) lamellae and mineralization is pyrite (py). Photograph by I.W. Honsberger. NRCan photo 2022-584; B) Scanning Electron Microscope image in Electron Backscatter mode of the Midway Gabbro mineral textures shown in A). bdy=baddeleyite. Photograph by M. Polivchuk. NRCan photo 2022-585.*

alteration is pervasive in the moderately altered gabbro west of Big Vein, whereas the Cracker gabbro is only very weakly altered to chlorite.

U–Pb BADDELEYITE GEOCHRONOLOGY

ANALYTICAL METHODS

The U–Pb baddeleyite dating of the Midway Gabbro was undertaken using ID-TIMS methods at the Jack Satterly Geochronology Laboratory, University of Toronto. Brown, platy laths and thick tabular crystals of baddeleyite (~80–110 microns long) lacking visible alteration were selected for analysis. Grains were cleaned at room temperature in 7N HNO_3 and Milli-Q water, and placed in Teflon capsules containing ~100 µL concentrated HF acid and 0.020 µL 7N HNO_3 for dissolution in a 200°C oven for 3 days. A $^{205}Pb/^{235}U$ ('ROM' in-house) spike was added to the dissolution capsules during sample loading. The solution was dried to a precipitate and re-dissolved in ~0.15 ml of 3N HCl overnight (Krogh, 1973). Uranium and Pb were isolated from the baddeleyite solution using 50 µL anion exchange columns with HCl, evaporated to a small droplet in H_3PO_4, deposited onto outgassed rhenium filaments with silica gel (Gerstenberger and Haase, 1997), and analyzed by a VG354 mass spectrometer using a Daly detector in pulse counting mode. All common Pb (0.3–0.5 pg) was assigned to procedural Pb blank. The dead time of the measuring system for Pb and U was 16 and 14 ns, respectively. The mass discrimination correction for the Daly detector was constant at 0.05% per atomic mass unit. Amplifier gains and Daly characteristics were monitored using the SRM 982 Pb standard. A thermal mass discrimination correction of 0.10% per atomic mass unit for Pb and U was used. Decay constants are those of Jaffey *et al.* (1971). All age errors are quoted in the text and Table 1, and error ellipses in the concordia diagram of Figure 3 are expressed at the 95% confidence interval. Plotting and age calculations used Isoplot 3.00 (Ludwig, 2003).

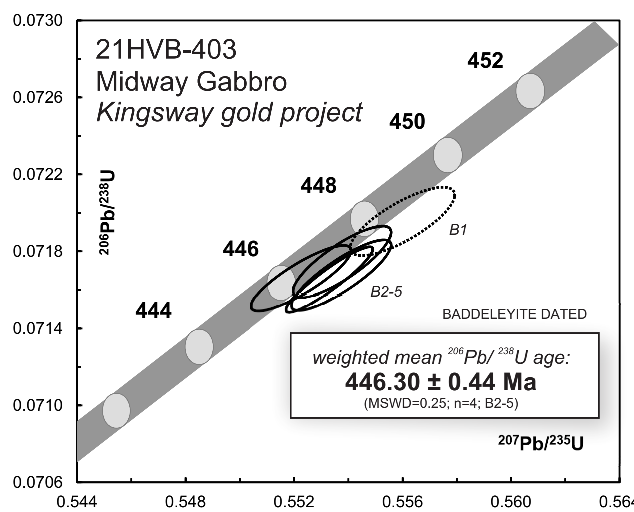

Figure 3. *Concordia plot of ID-TIMS U–Pb baddeleyite dates for the Midway Gabbro (21HVB-403). The weighted mean $^{206}Pb/^{238}U$ age of the youngest four baddeleyite analyses is 446.30 ± 0.44 Ma, which is interpreted to represent the closest minimum age estimate for crystallization of the Midway Gabbro.*

Table 1. Isotope dilution-thermal ionization mass spectrometry U–Pb isotopic baddeleyite data for the Midway Gabbro, Labrador Gold Corporation's Kingsway gold project

Mineral/ Analysis No.	Weight (µg)	U (ppm)	Th/U	Pbc (pg)	$^{206}Pb/^{204}Pb$ measured	$^{207}Pb/^{235}U$	2σ	$^{206}Pb/^{238}U$	2σ	Error Corr	$^{207}Pb/^{206}Pb$	2σ	Age (Ma) $^{206}Pb/^{238}U$	2σ	Age (Ma) $^{207}Pb/^{235}U$	2σ	Age (Ma) $^{207}Pb/^{206}Pb$	2σ	% Disc
B1	0.005	134	0.06	0.4	7732	0.5560	0.0016	0.071959	0.00015	0.776	5.60E-02	1.01E-04	447.95	0.87	448.93	1.03	453.95	4.0	1.4
B2	0.001	851	0.09	0.4	10744	0.5538	0.0015	0.071749	0.00015	0.826	5.60E-02	8.49E-05	446.68	0.91	447.47	0.97	451.50	3.4	1.1
B3	0.001	564	0.07	0.4	6399	0.5538	0.0015	0.071679	0.00015	0.853	5.60E-02	8.00E-05	446.27	0.90	447.45	0.98	453.60	3.2	1.7
B4	0.001	831	0.11	0.5	7487	0.5523	0.0015	0.071664	0.00014	0.849	5.59E-02	8.00E-05	446.17	0.84	446.48	0.98	448.00	3.3	0.4
B5	0.004	666	0.10	0.3	38459	0.5533	0.0013	0.071657	0.00014	0.927	5.60E-02	5.00E-05	446.13	0.84	447.16	0.85	452.45	2.0	1.4

Notes:
B is baddeleyite.
Th/U calculated from radiogenic $^{208}Pb/^{206}Pb$ ratio and $^{207}Pb/^{206}Pb$ age assuming concordance.
Pbc is total common Pb assuming the isotopic composition of laboratory blank: ($^{206}Pb/^{204}Pb$=18.49 ± 0.4%; $^{207}Pb/^{204}Pb$=15.59 ± 0.4%; $^{208}Pb/^{204}Pb$=39.36 ± 0.4%).
$^{206}Pb/^{204}Pb$ corrected for fractionation and common Pb in the spike.
Pb/U ratios corrected for fractionation, common Pb in the spike, and blank.
Correction for ^{230}Th disequilibrium in $^{206}Pb/^{238}U$ and $^{207}Pb/^{206}Pb$ assuming Th/U of 4.2 in the magma.
Disc is percent discordance for the given $^{207}Pb/^{206}Pb$ age.
Error Corr is correlation coefficients of X-Y errors on the concordia plot.
Decay constants are those of Jaffey *et al.* (1971): ^{238}U and ^{235}U are 1.55125 X 10-10/yr and 9.8485 X 10-10/yr.
$^{238}U/^{235}U$ ratio of 137.88 used for $^{207}Pb/^{206}Pb$ model age calculations.

RESULTS

Five U–Pb results from single grains, or groups of 2–3 grains, gave overlapping data that are concordant or plot just to the right of the curve. The weighted mean $^{206}Pb/^{238}U$ age obtained from the tight cluster of 4 results (B2-5) is 446.30 ± 0.44 Ma (MSWD=0.25). This age can be considered a minimum age for the time of gabbro emplacement. One result (B1) is slightly older with a $^{206}Pb/^{238}U$ date of 448 Ma and may indicate that the gabbro is slightly older if B2–B5 have lost a minor amount of Pb in equal measure. A maximum age estimate is given by the mean $^{207}Pb/^{206}Pb$ age of B1–5 of 452 ± 1 Ma. However, given the partial concordance and high degree of overlap of our results, our preferred interpretation is that 446.30 ± 0.44 Ma represents the closest age estimate for crystallization of the gabbro.

LITHOGEOCHEMISTRY

METHODS

Eight, ~1 to 2 kg, whole-rock samples from seven different intrusions were prepared for lithogeochemical analyses (Appendix A). All samples were crushed to ~1 cm rock chips and then pulverized in a mild steel shatter box. These samples were processed and analyzed by ALS Geochemistry Laboratories (www.alsglobal.com), Sudbury, Ontario, for eleven major elements and fifty-four minor and trace elements, including Au and Ag (Appendix A). Solutions of crushed and powdered samples were prepared for chemical analyses using lithium borate fusion and acid dissolution. Major elements were analyzed by inductively coupled plasma-atomic emission spectrometry (ICP-AES) and most minor and trace elements by inductively coupled plasma-mass spectrometry (ICP-MS). The following metals were analyzed by applying four acid digestion and ICP-AES: Ag, Cd, Co, Cu, Li, Mo, Ni, Pb, Sc and Zn. Infrared spectroscopy was used to analyze for C and S, with atomic absorption spectrometry used to analyze Au.

The eight additional samples were processed and analyzed at the geochemical laboratory of the Geological Survey of Newfoundland and Labrador (GSNL) in St. John's, Newfoundland following the methods outlined in Finch *et al.* (2018) (Appendix B). Major elements were analyzed by inductively coupled plasma-optical emission spectrometry (ICP-OES) following borate fusion. FeO was determined through titration, $Fe_2O_3^T$ is the total iron as ferric oxide, and Fe_2O_3 was calculated from the other two iron analyses. Loss on ignition (LOI) was obtained using gravimetric analysis. Trace elements were determined using both ICP-MS following borate fusion, and

ICP-OES following four-acid digestion. Silver was determined through ICP-OES following nitric acid digestion. An ion selective electrode (ISE) was used to analyze for fluoride. A suite of 27 elements was analyzed by Instrumental Neutron Activation Analysis (INAA) at Bureau Veritas Laboratories (https:// www.bvlabs. com). Major elements are reported in weight % and trace elements are reported in ppm with the exception of Au, which is given in ppb. Negative detection limit values represent analyses below the detection limit and -99 represents samples that were not analyzed for that element. Information on quality assurance and quality control (QA/QC) procedures with respect to the reference materials are in the appendices of Finch *et al.* (2018).

RESULTS

Lithogeochemical data for the eleven gabbro intrusions (16 samples) are presented in Appendices A and B and plotted in Figures 4–6. Comparative data include gabbro of the Mount Peyton Intrusive Suite (Sandeman *et al.*, 2017; Figure 1) and weakly mineralized to unaltered gabbro intrusions east of Duder Lake (Churchill, 1994). The whole-rock compositions of the eleven gabbro intrusions range from picro-basalt and basalt to basaltic-andesite and basaltic-trachyandesite with respect to their total alkali and silica contents (Figure 4A), and range between subalkaline basalt and basaltic andesite in the immobile trace-element classification plot (Figure 4B; Pearce, 1996). The Mount Peyton and Duder Lake comparative datasets span the compositional range of the gabbro samples, and also extend to higher silica contents (Figure 4).

The multi-element patterns for the gabbros along the Dog Bay Line–Appleton Fault Zone gold corridor are variable but can be grouped broadly into two types. Type 1 - minor enrichment in light rare-earth elements (LREE) and large-ion lithophile elements (LILE), relative to the heavy-rare-earth elements (HREE) and variably developed high-field-strength-element (HFSE: Nb, P, Zr-Hf, Ti) troughs; and Type 2 - modest to significant enrichment in LREE and LILE and also variably developed HFSE troughs (Figure 5). Type 1 gabbros consist of the Lucky Moose gabbro, the gabbro west of Big Vein, and one of the intrusions to the north-northwest of the Midway Gabbro, whereas Type 2 gabbros consist of the Cracker gabbro, Midway Gabbro, one of the intrusions to the north-northwest of Midway, Titan gabbro, and Road Breccia gabbro (Figure 5). The Midway Gabbro, Titan gabbro, and one of the intrusions to the northwest of Midway display significant LREE and LILE enrichment, whereas the gabbro west of Big Vein and the Road Breccia gabbro (Figure 2) have moderate LREE and LILE enrichment. The Midway and Titan gabbros have the steepest REE patterns and the highest La/Sm (Figure 5A). Mount Peyton Intrusive Suite gabbro multi-element patterns are more sim-

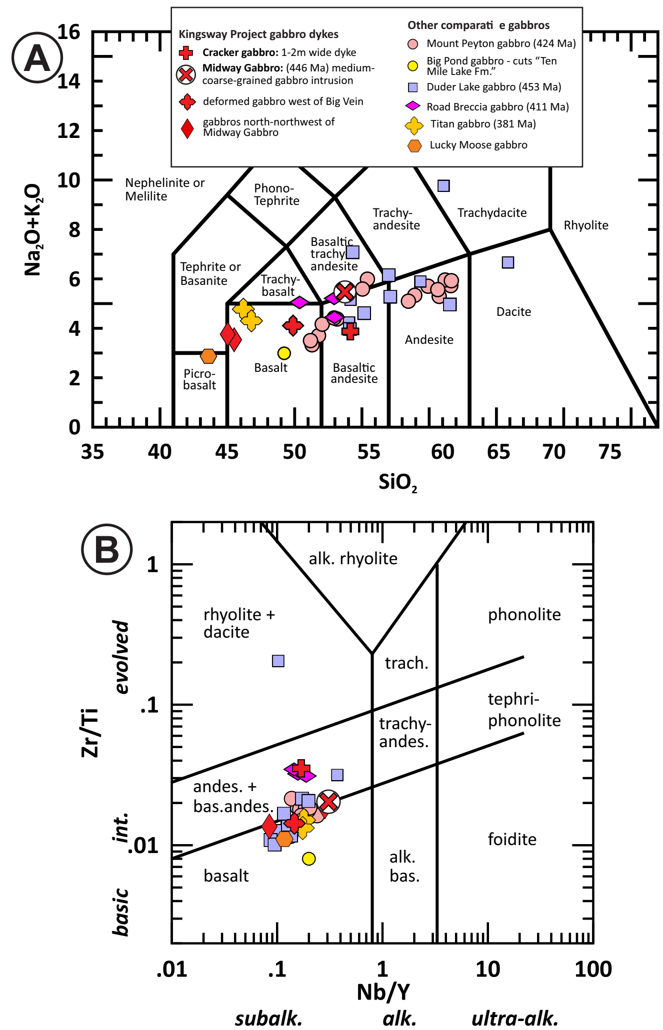

Figure 4. *Plots of lithogeochemical data for gabbro intrusions along the Dog Bay Line–Appleton Fault Zone gold corridor. Comparative datasets are presented for gabbro of the Mount Peyton Intrusive Suite (pink circles; Sandeman* et al.*, 2017) and gabbro intrusions east of Duder Lake (purple squares). The Duder Lake data are from Churchill (1994), and also include our four Corvette and Goldstash gabbro samples. A) SiO_2* vs. *$Na_2O + K_2O$ (wt. %) classification diagram (LeBas* et al.*, 1986); B) Nb/Y* vs. *Zr/Ti (ppm) classification plot (Pearce, 1996).*

ilar to Type 2 gabbros, whereas the Big Pond gabbro is transitional between Type 1 and Type 2 (Figure 5). The Duder Lake gabbros are similar to Type 1 as they are less enriched in LREE than the Type 2 Cracker, Midway, and Road Breccia gabbros.

The gabbro west of Big Vein and one of the intrusions to the north-northwest of the Midway Gabbro exhibit minor positive Eu anomalies, whereas all the other data, except the Road Breccia gabbro, lack Eu anomalies (Figure 5A, C).

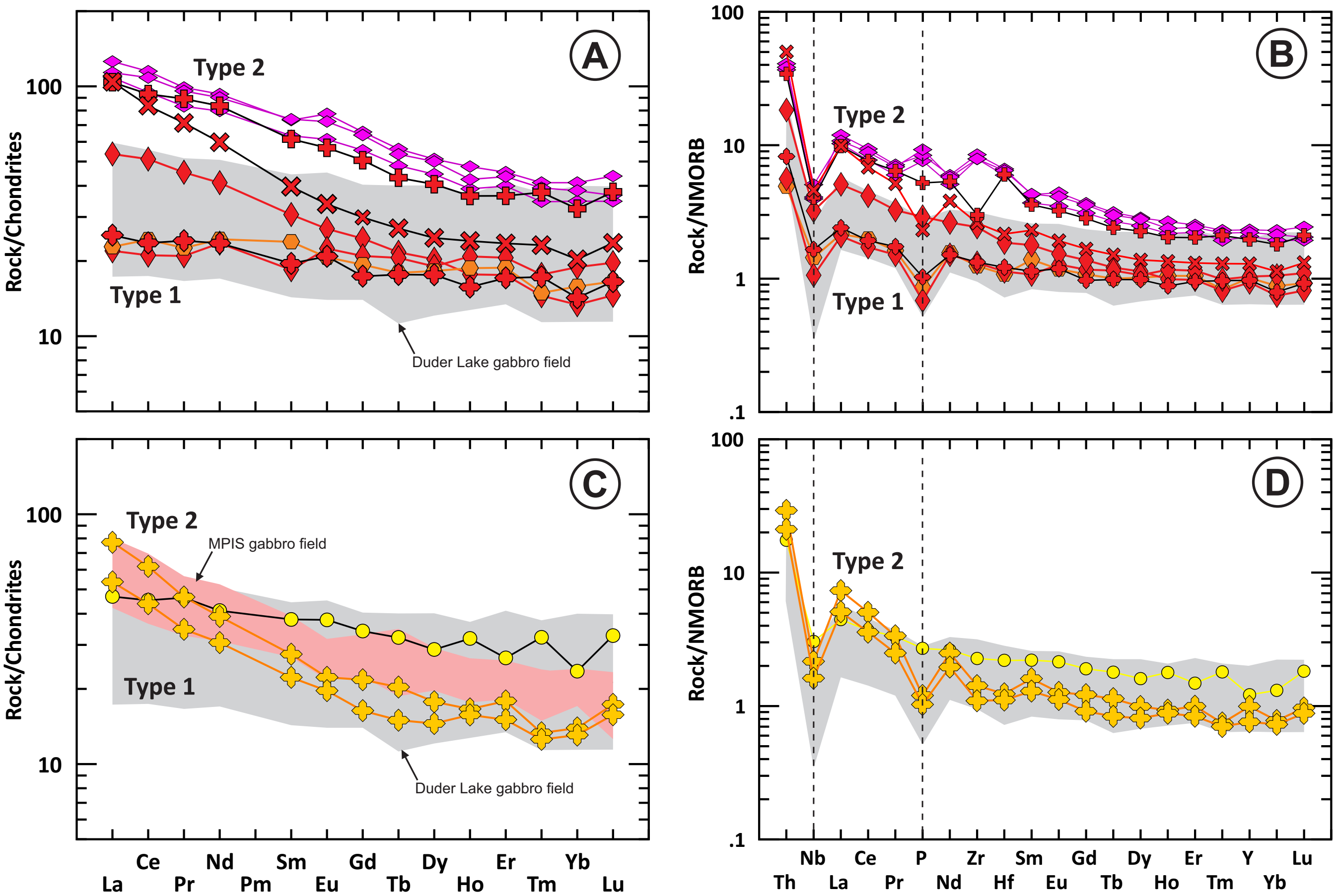

Figure 5. *Multi-element plots. A) Data normalized to chondrite; B) Data normalized to NMORB. Chondrite and NMORB values utilized are from Sun and McDonough (1989). Type 2 gabbros are enriched in light rare-earth elements and large-ion lithophile elements relative to Type 1. Symbols as in Figure 4.*

Type 2 gabbros display prominent negative Nb anomalies with respect to Th and La, whereas the negative Nb anomalies for Type 1 gabbros are more modest (Figure 5B, D). Modest to prominent negative P anomalies are apparent in most samples with the exception of the Cracker gabbro, one of the intrusions north-northwest of Midway, and the Big Pond and Road Breccia gabbros. The Road Breccia gabbro displays minor positive Eu and P anomalies and has a modest positive Zr–Hf anomaly (Figure 5A, B).

The petrochemistry of the gabbro intrusions along the Dog Bay Line–Appleton Fault Zone gold corridor is further examined using minor- and trace-element tectonic discrimination diagrams (Figure 6). On the $Zr/(P_2O_5*10^4)$ *vs.* TiO_2 diagram (Floyd and Winchester, 1975; Winchester and Floyd, 1977), all gabbros are tholeiitic basalts except the Road Breccia gabbro, which is an alkali basalt (Figure 6A). The gabbros span the back-arc basin basalt (BAB) – mid-ocean ridge basalt (MORB) and alkaline basalt fields on the Ti/1000 *vs.* V diagram (Shervais, 1982), with Road Breccia, Big Pond, Cracker, Midway, and one gabbro north-northwest of Midway being alkaline basalts (Figure 6B). All the gabbros are arc basalts on the Th *vs.* Nb/16 *vs.* Zr/117 diagram (Figure 6C; Wood, 1980). Type 1 and Type 2 gabbros recognized from multi-element patterns are spatially distinct on the La/10 *vs.* Nb/8 *vs.* Y/15 diagram (Figure 6D; Cabanis and Lecolle, 1989). Type 1 gabbros are back-arc basin basalts, whereas Type 2 gabbros straddle the boundaries between the continental basalt field and calc-alkaline and transitional arc basalt fields (Figure 6D). The Mount Peyton gabbro plot co-spatially with Type 2 gabbros, whereas the Duder Lake gabbro are co-spatial with Type 1 gabbros (Figure 6D).

The Nb/Yb *vs.* Th/Yb diagram is utilized for discriminating interaction of Th-enriched continental crust or lithospheric mantle with asthenosphere-derived basaltic melts (Figure 6E; Pearce, 2008). All the gabbro intrusions have moderately elevated Th/Yb ratios that lie above the asthenospheric mantle array, consistent with Th contribution from subduction zone magmatism or through the interaction of asthenosphere-derived basalt with crust and/or litho-

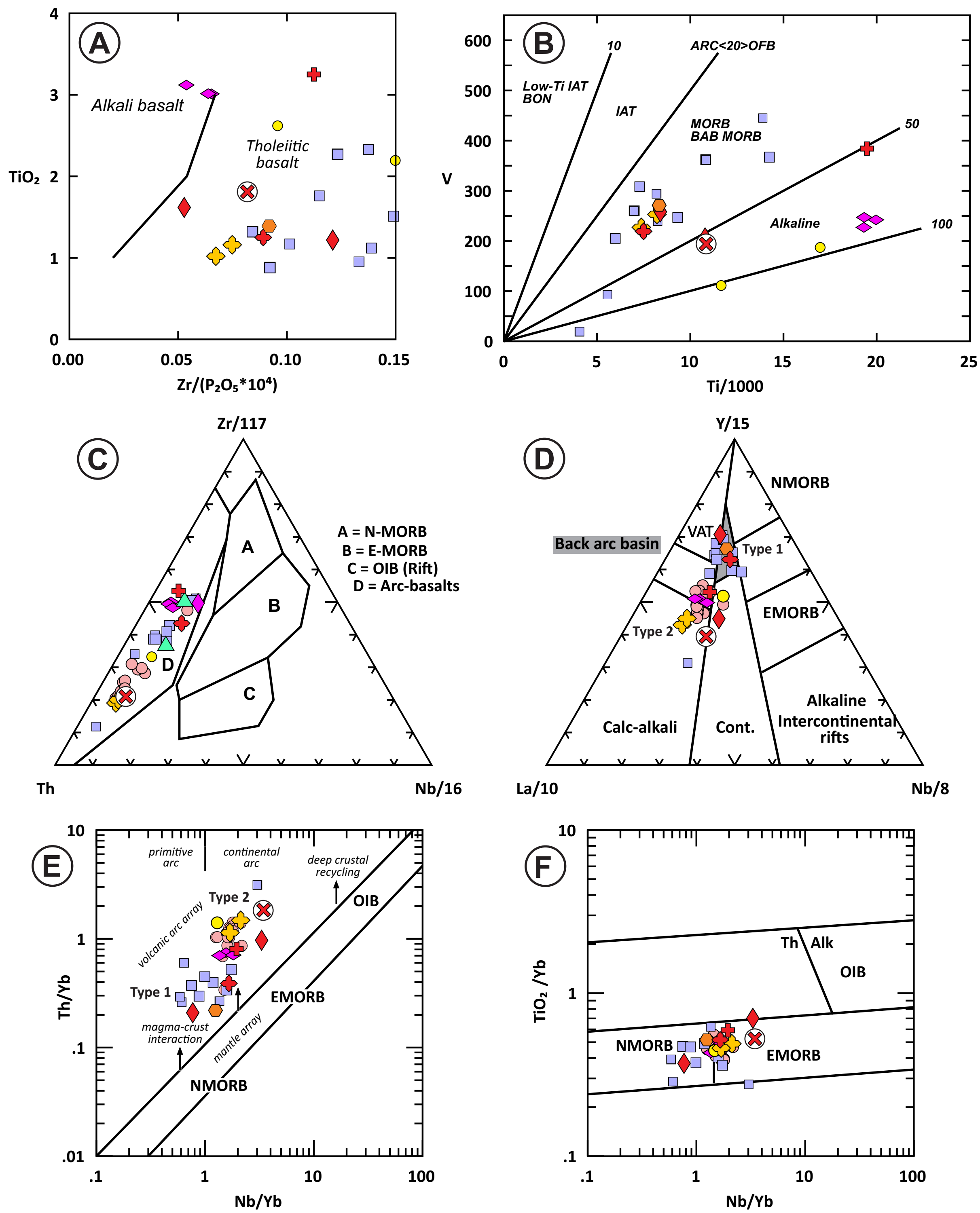

Figure 6. *Tectonic discrimination diagrams. A) $Zr/(P_2O_5*104)$* vs. *TiO_2 (Floyd and Winchester, 1975; Winchester and Floyd, 1977); B) Ti/1000* vs. *V (Shervais, 1982); C) Th* vs. *Nb/16* vs. *Zr/117 (Wood, 1980); D) La/10* vs. *Nb/8* vs. *Y/15 (Cabanis and Lecolle, 1989); E) Nb/Yb (ppm)* vs. *Th/Yb (Pearce, 2008); F) Nb/Yb* vs. *TiO_2/Yb (Pearce, 2008). Symbols as in Figure 4. Abbreviations: Alk/alk–alkaline; BAB–back arc basin; Bon–boninite; Cont.–continental; EMORB–enriched mid-ocean ridge basalt; IAT–island arc tholeiite; MORB–mid-ocean ridge basalt; MPIS–Mount Peyton Igneous Suite; NMORB–normal mid-ocean ridge basalt; OFB–ocean floor basalt; OIB–ocean island basalt; subalk.–subalkaline; Th–tholeiitic; VAT–volcanic arc tholeiite.*

sphere (Figure 6E). Type 2 gabbros are more enriched in Th/Yb relative to Type 1 gabbros, with the Midway Gabbro having the highest Th/Yb and Nb/Yb ratios (Figure 6E). The Nb/Yb *vs.* TiO_2/Yb diagram is a companion to the Nb/Yb *vs.* Th/Yb diagram and is utilized to assess the depth of melting as a function of TiO_2 (Figure 6F; Pearce, 2008). All the studied gabbros have relatively low TiO_2/Yb ratios and plot in the shallow-melting, asthenospheric array, with Type 1 gabbros reflecting slightly shallower melting of more depleted asthenosphere than Type 2 gabbros (Figure 6F).

DISCUSSION

The 446.30 ± 0.44 Ma (Late Ordovician, Katian) $^{206}Pb/^{238}U$ baddeleyite age (Figure 3 and Table 1) is considered a minimum age for the time of emplacement of the Midway Gabbro. One baddeleyite grain is slightly older (448 Ma) and may indicate that the gabbro is slightly older if the four youngest baddeleyite grains lost the same minor amount of Pb (Figure 3). The new Katian age is consistent with the intrusion of the Midway Gabbro into clastic sedimentary rocks of the Ordovician Davidsville Group (Currie, 1995a, b; Dickson, 2006; Dickson *et al.*, 2007) and places a maximum age constraint on the timing of orogenic gold mineralization along the Dog Bay Line–Appleton Fault Zone gold corridor. The 446 Ma minimum baddeleyite age is just slightly younger than the *ca.* 453 Ma baddeleyite age for the gabbro intrusion east of Duder Lake that hosts the Corvette gold prospect (Dickson *et al.*, 2007), and much older than the *ca.* 381 Ma zircon age for the Titan gabbro gold prospect that intrudes the Silurian Indian Islands Group (McNicoll *et al.*, 2006).

The gabbro intrusions along the Dog Bay Line–Appleton Fault Zone gold corridor are grouped broadly into two lithogeochemical types. Type 1 gabbros have minor to no enrichment in LREE and LILE relative to the HREE, and include a gabbro north-northwest of the Midway Gabbro, a gabbro west of Big Vein, the Lucky Moose gabbro gold showing north of the Kingsway project, and the Duder Lake gabbro intrusions (Figures 4–6). These gabbros are hypabyssal, back-arc basin tholeiites derived from relatively depleted, peridotitic source(s). Type 2 gabbros are moderately to significantly enriched in LREE, LILE, and Th and include the Midway, Cracker, Titan, Road Breccia, Big Pond and Mount Peyton gabbros, as well as one gabbro north-northwest of Midway (Figures 4–6). These hypabyssal gabbros are "arc-like", calc-alkaline to transitional intrusions derived from peridotitic source(s) that strongly interacted with the crust and/or lithosphere. Negative Nb anomalies for both types of gabbros imply formation by partial melting of hydrated and metasomatized subducted lithosphere (*e.g.*, Green, 1995; Tiepolo *et al.*, 2001; Grove *et al.*, 2003; Larocque and Canil, 2010; Grove and Brown, 2018); however, Type 1 melts were less influenced by subducted lithosphere (Figures 5 and 6E).

The gabbro intrusions along the Dog Bay Line–Appleton Fault Zone gold corridor that are constrained by U–Pb geochronology include the Corvette (Duder Lake; *ca.* 453 Ma, Dickson *et al.*, 2007), Midway (*ca.* 446 Ma, *this study*), Mount Peyton (*ca.* 424–418 Ma, Sandeman *et al.*, 2017), Road Breccia (*ca.* 411 Ma, McNicoll *et al.*, 2006), and Titan (*ca.* 381 Ma, McNicoll *et al.*, *ibid.*) gabbro gold showings. Late Ordovician Type 1 (Corvette/Duder Lake) and Type 2 (Midway) gabbros were both emplaced potentially as a result of extension in the intra-oceanic Tetagouche–Exploits back-arc basin (*e.g.*, Zagorevski *et al.*, 2007). Juxtaposition of different clastic sedimentary rock slices containing lithogeochemically distinct Late Ordovician gabbros is consistent with post-Ordovician imbrication of sedimentary–igneous rock sequences along the Dog Bay Line–Appleton Fault Zone gold corridor (Figure 2), complicating correlations between lithogeochemistry and geochronology.

The remaining gabbro ages along the Dog Bay Line–Appleton Fault Zone gold corridor come from Silurian to Devonian gabbro intrusions that are all lithogeochemically classified as Type 2. The Ludlow–Pridoli Mount Peyton gabbros are interpreted as post-Salinic, intracontinental, extension-related, lithospheric melts that formed during slab roll-back and/or break-off (van Staal *et al.*, 2014; Sandeman *et al.*, 2017; Honsberger *et al.*, 2022a, b), whereas the Early Devonian Road Breccia and Late Devonian Titan gabbros may represent lithospheric melts associated with the Acadian orogenic cycle (McNicoll *et al.*, 2006; Dickson *et al.*, 2007). The *ca.* 411 Ma (Road Breccia) and *ca.* 381 Ma (Titan) gabbro ages fall within the time periods of two major orogenic gold-forming events in Newfoundland (433–405 and 390–372 Ma) that are associated with deformation immediately preceding, and during, the Acadian orogenic cycle (Sandeman *et al.*, 2022). Overall, geochronological and lithogeochemical constraints on gabbro intrusions along the Dog Bay Line–Appleton Fault Zone gold corridor are consistent with a polyphase tectonomagmatic history that spans the Late Ordovician to Devonian, with reactivation of structures as strike-slip faults likely in the Late Devonian and Carboniferous.

CONCLUSIONS

A new high-precision ID-TIMS U–Pb minimum baddeleyite age of 446.30 ± 0.44 Ma is reported for an auriferous gabbro intrusion, the Midway Gabbro, on Labrador Gold Corporation's Kingsway gold project. This new Katian age places a maximum age constraint on post-intrusion, gabbro-hosted orogenic gold mineralization along the Dog Bay Line–Appleton Fault Zone gold corridor.

The different hypabyssal gabbro intrusions along the Dog Bay Line–Appleton Fault Zone gold corridor can be separated broadly into two lithogeochemical types. Type 1 gabbros are tholeiitic back-arc basin magmas with minor to no enrichment in LREE and LILE relative to the HREE. Type 2 gabbros are transitional to calc-alkaline, arc-like magmas with modest to significant enrichment in LREE and LILE. There are both Type 1 and Type 2 gabbro intrusions of Late Ordovician age along the Dog Bay Line–Appleton Fault Zone gold corridor, whereas all known Silurian to Devonian gabbro intrusions in the area are Type 2. Late Ordovician Type 1 and Type 2 gabbros may have formed in the intra-oceanic Tetagouche–Exploits back-arc basin. Late Silurian to Devonian Type 2 gabbros likely formed during post-Salinic extension and subsequent Acadian orogenesis associated with orogenic gold mineralization.

Gabbro intrusions along the Dog Bay Line–Appleton Fault Zone gold corridor record a polyphase tectonomagmatic history that spans the Late Ordovician to Devonian. Structural juxtaposition of gabbro intrusions of varying age and lithogeochemical characteristics implies that sedimentary–igneous rock sequences were imbricated and dismembered along the Dog Bay Line–Appleton Fault Zone gold corridor during the Acadian and Neo-Acadian orogenic cycles that likely culminated with Carboniferous transpressional– transtensional strike-slip.

ACKNOWLEDGMENTS

This collaborative research between the Geological Survey of Canada and Geological Survey of Newfoundland and Labrador is part of Natural Resources Canada's Targeted Geoscience Initiative 6. Many thanks to Labrador Gold Corporation, New Found Gold Corporation, and Exploits Gold Corporation for property tours, core viewing, and sampling opportunities, as well as M. Polivchuk for SEM analyses and images. H. Sandeman acknowledges the help and hard work of the staff at the Geological Survey of Newfoundland and Labrador, Geochemical Laboratory, colleagues J. Rooney and H. Campbell, and field assistants T. Nickson, T. Mugford, and M. O'Neill. Reviews by John Hinchey and Jennifer Smith-Holder are appreciated. This is Natural Resources Canada Contribution Number 20220561.

REFERENCES

Cabanis, B. and Lecolle, M.
1989: Le diagramme La/10-Y/15-Nb/8: un outil pour la discrimination des séries volcaniques et la mise en évidence des processus de mélange et/ou de contamination crustale: Comptes rendus de l'Académie des sciences, Série 2, Mécanique, Physique, Chimie, Sciences de l'univers, Sciences de la Terre, Volume 309, pages 2023-2029.

Churchill, R.A.
1994: An integrated study of epigenetic gold mineralization, Duder Lake area, northeastern Newfoundland. Unpublished M.Sc. thesis, Memorial University of Newfoundland, St. John's, Newfoundland.

Churchill, R.A. and Evans, D.T.W.
1992: Geology and gold mineralization of the Duder Lake gold showings, eastern Notre Dame Bay, Newfoundland. *In* Current Research. Government of Newfoundland and Labrador, Department of Mines and Energy, Geological Survey Branch, Report 92-1, pages 211-220.

Churchill, R.A., Wilton, D.H.C. and Evans, D.T.W.
1993: Geology, alteration assemblages and geochemistry of the Duder Lake gold showings, northeastern Newfoundland. *In* Current Research. Government of Newfoundland and Labrador Department of Mines and Energy, Geological Survey Branch, Report 93-1, pages 317-333.

Colman-Sadd, S., Hayes, J. and Knight, I.
1990: The geology of the Island of Newfoundland. Government of Newfoundland and Labrador, Department of Mines and Energy, Geological Survey Branch, Map 90-01, Scale: 1:1 000 000

Currie, K.L.
1993: Ordovician-Silurian stratigraphy between Gander Bay and Birchy Bay, Newfoundland. Geological Survey of Canada, Paper 931D, pages 1118.

1995a: Geology, Gander River, Newfoundland, Geological Survey of Canada, Open File 3162, scale 1:50 000.

1995b: The northeastern end of the Dunnage Zone in Newfoundland. Atlantic Geology, Volume 31, pages 25-38.

Dickson, W.L.
2006: The Silurian Indian Islands Group and its relationships to adjacent units. *In* Current Research. Government of Newfoundland and Labrador, Department of Natural Resources, Geological Survey, Report 06-1, pages 1-24.

Dickson, W.L., Colman-Sadd, S.P. and O'Brien, B.H.
2000: Geology of the Botwood map area (NTS 2E/3),

central Newfoundland. Map 2000-11. Government of Newfoundland and Labrador, Department of Mines and Energy, Geological Survey, Open File 2E/03/1067 Version 2.0.

Dickson, W.L., McNicoll, V.J., Nowlan, G.S. and Dunning, G.R.
2007: The Indian Islands Group and its relationships to adjacent units: recent data. *In* Current Research. Government of Newfoundland and Labrador, Department of Natural Resources, Geological Survey, Report 07-1, pages 1-9.

Evans, D.T.W.
1996: Epigenetic gold occurrences, eastern and central Dunnage Zone, Newfoundland. Government of Newfoundland and Labrador, Department of Mines and Energy, Geological Survey, Mineral Resources Report 9, 135 pages.

Evans, D.T.W. and Hayes, J.P.
1992: Gander River. Government of Newfoundland and Labrador, Department of Mines and Energy, Geological Survey Branch, Open File 2E/02/0839.

Finch, C., Roldan, R., Walsh, L., Kelly, J. and Amor, S.
2018: Analytical methods for chemical analysis of geological materials. Government of Newfoundland and Labrador, Department of Natural Resources, Geological Survey, Open File NFLD/3316, 67 pages.

Floyd, P.A. and Winchester, J.A.
1975: Magma type and tectonic setting discrimination using immobile elements. Earth and Planetary Science Letters, Volume 27, pages 211-218. http://dx.doi.org/10.1016/0012-821X(75)90031-X

Gerstenberger, H. and Haase, G.
1997: A highly effective emitter substance for mass spectrometric Pb isotope ratio determinations. Chemical Geology, Volume 136, pages 309-312.

Green, T.H.
1995: Significance of Nb/Ta as an indicator of geochemical processes in the crust-mantle system. Chemical Geology, Volume 120, Issues 3-4, pages 347-359.

Grove, T.L. and Brown, S.M.
2018: Magmatic processes leading to compositional diversity in igneous rocks: Bowen (1928) revisited. American Journal of Science, Volume 318, Number 1, pages 1-28.

Grove, T.L., Elkins-Tanton, L.T., Parman, S.W., Chatterjee, N., Meuntener, O. and Gaetani, G.A.
2003: Fractional crystallization and mantle melting controls on calc-alkaline differentiation trends. Contributions to Mineralogy and Petrology, Volume 145, Number 5, pages 515-533.

Honsberger, I.W., Bleeker, W., Kamo, S.L., Sandeman, H.A.I., Evans, D.T.W., van Staal, C.R., Rogers, N. and Dunning, G.R.
2022a: Latest Silurian syntectonic sedimentation and magmatism and Early Devonian orogenic gold mineralization, central Newfoundland Appalachians, Canada: Setting, structure, lithogeochemistry, and high-precision U–Pb geochronology. Geological Society of America Bulletin. https://doi.org/10.1130/B36083.1.

Honsberger, I.W., Bleeker, W., Kamo, S.L., Sutcliffe, C.N. and Sandeman, H.A.I.
2022b: U–Pb geochronology of Late Silurian (Wenlock to Pridoli) volcanic and sedimentary rocks, central Newfoundland Appalachians: Targeting the timing of transient extension as a prelude to Devonian orogenic gold mineralization. Atlantic Geoscience, Volume 58, pages 215-237.

Jaffey, A.H., Flynn, K.F., Glendenin, L.E., Bentley, W.C. and Essling, A.M.
1971: Precision measurement of half-lives and specific activities of ^{235}U and ^{238}U. Physical Review C, Volume 4, page 1889.

Krogh, T.E.
1973: A low-contamination method for hydrothermal decomposition of zircon and extraction of U and Pb for isotopic age determinations. Geochimica et Cosmochimica Acta, Volume 37, Number 3, pages 485-494.

Larocque, J. and Canil, D.
2010: The role of amphibole in the evolution of arc magmas and crust: The case from the Jurassic Bonanza arc section, Vancouver Island, Canada. Contributions to Mineralogy and Petrology, Volume 159, pages 475-492. doi:10.1007/s00410-009-0436-z

LeBas, M., Maitre, R.L., Streckeisen, A. and Zanettin, B.
1986: IUGS Subcommission on the systematics of igneous rocks; a chemical classification of volcanic rocks based on the total alkali-silica diagram. Journal of Petrology, Volume 27, Number 3, pages 745-750.

Lincoln, N., Farmer, R., Eccles, R. and Deering, P.D.
2018: Preliminary economic assessment of the Valentine Lake gold project Newfoundland, Canada;

Marathon Gold. <www.marathongold.com/site/assets/files/5047/2018-10-pea.pdf> [accessed December 2, 2018]

Ludwig, K.
2003: Isoplot 3.00: A geochronological toolkit for Microsoft Excel.

McNicoll, V.J., Squires, G.C., Wardle, R.J., Dunning, G.R. and O'Brien, B.H.
2006: U–Pb geochronological evidence for Devonian deformation and gold mineralization in the eastern Dunnage Zone, Newfoundland. *In* Current Research. Government of Newfoundland and Labrador, Department of Natural Resources, Geological Survey, Report 06-1, pages 45-60.

Moss, R.
2022: Labrador Gold Corp., Kingsway Gold Project, unpublished Corporate Update, 29 pages.

O'Brien, B.H.
2003: Geology of the central Notre Dame Bay region (parts of NTS areas 2E/3, 6, 11), northeastern Newfoundland. Government of Newfoundland and Labrador, Department of Mines and Energy, Geological Survey Branch, Report 03-03, 147 pages.

Pearce, J.A.
1996: A user's guide to basalt discrimination diagrams. Geological Association of Canada, Short Course Notes, Volume 12, pages 79-113.

2008: Geochemical fingerprinting of oceanic basalts with applications to ophiolite classification and the search for Archean oceanic crust. Lithos, Volume 100, pages 14-48.

Piasecki, M.A.J.
1992: Tectonics across the Gander-Dunnage boundary in northeastern Newfoundland. *In* Current Research, Part E. Geological Survey of Canada, Paper 92-JE, pages 259-268.

Pollock, J.C., Wilton, D.H.C., van Staal, C.R. and Morrissey, K.D.
2007: U–Pb detrital zircon geochronological constraints on the Early Silurian collision of Ganderia and Laurentia along the Dog Bay Line: The terminal Iapetan suture in the Newfoundland Appalachians. American Journal of Science, Volume 307, pages 399-433.

Reusch, D.N. and van Staal, C.R.
2012: The Dog Bay–Liberty Line and its significance for Silurian tectonics of the northern Appalachian orogen: Canadian Journal of Earth Sciences, Volume 49, pages 239-258.

Sandeman, H.A.I., Dunning, G.R., McCullough, C.K. and Peddle, C.
2017: U–Pb geochronology, petrogenetic relationships and intrusion-related precious-metal mineralization in the northern Mount Peyton Intrusive Suite: implications for the origin of the Mount Peyton trend, central Newfoundland (NTS 2D/04). In Current Research. Government of Newfoundland and Labrador, Department of Natural Resources, Geological Survey, Report 17-1, pages 189-217.

Sandeman, H.A.I., Honsberger, I.W. and Camacho, A.
2022: Overview of age constraints for gold mineralization in central and western Newfoundland and new $^{40}Ar/^{39}Ar$ ages for white mica from selected auriferous zones. Atlantic Geoscience, Volume 58. https://doi.org/10.4138/atlgeo.2022.010.

Shervais, J.W.
1982: Ti-V plots and the petrogenesis of modern and ophiolitic lavas. Earth and Planetary Science Letters, Volume 59, pages 101-118.

Squires, G.C.
2005: Gold and antimony occurrences of the Exploits Subzone and Gander Zone: A review of recent discoveries and their interpretations. *In* Current Research. Government of Newfoundland and Labrador, Department of Natural Resources, Geological Survey, Report 05-1, pages 223-237.

Srivastava, R.M.
2022: Exploration update of the Queensway project, Newfoundland and Labrador, Canada. Amended and Restated National Instrument 43-101 Technical Report. Prepared by RedDot3D Inc. on behalf of New Found Gold Corp., 260 pages.

Strong, D.F.
1979: The Mount Peyton Batholith, central Newfoundland, a bi-modal calc-alkaline suite. Journal of Petrology, Volume 20, pages 119-138.

Sun, S.S. and McDonough, W.F.
1989: Chemical and isotopic systematics of oceanic basalts: implications for mantle composition and processes. *In* Magmatism in the Ocean Basin. *Edited by*

A.D. Saunders and M.J. Norry. Geological Society of London, Special Publication 42, pages 313-345.

Tiepolo, M., Bottazzi, P., Foley, S.F., Oberti, R., Vannucci, R. and Zanetti, A.
2001: Fractionation of Nb and Ta from Zr and Hf at mantle depths: The role of titanian pargasite and kaersutite. Journal of Petrology, Volume 42, Issue 1, pages 221-232.

Tuach, J., Dean, P.L, Swinden, H.S., O'Driscoll, C.F., Kean, B.F. and Evans, D.T.W.
1988: Gold mineralization in Newfoundland: A 1988 review. *In* Current Research. Government of Newfoundland and Labrador, Department of Mines, Mineral Development Division, Report 88-1, pages 279-306.

Valverde-Vaquero, P., van Staal, C.R., McNicoll, V. and Dunning, G.R.
2006: Mid–Late Ordovician magmatism and metamorphism along the Gander margin in central Newfoundland. Journal of the Geological Society of London, Volume 163, pages 347-362.

van Staal, C.R., Zagorevski, A., McNicoll, V.J. and Rogers, N.
2014: Time-transgressive Salinic and Acadian orogenesis, magmatism, and Old Red Sandstone sedimentation in Newfoundland. Geoscience Canada, Volume 41, pages 138-164.

Williams, H.
1993: Stratigraphy and structure of the Botwood Belt and definition of the Dog Bay Line in northeastern Newfoundland. *In* Current Research, Part D. Geological Survey of Canada, Paper 93-1D, pages 19-27.

Williams, H., Colman-Sadd, S.P. and Swinden, H.S.
1988: Tectonic-stratigraphic subdivisions of central Newfoundland. *In* Current Research, Part B. Geological Survey of Canada, Paper 88-1B, pages 91-98.

Williams, H., Currie, K.L. and Piasecki, M.A.J.
1993: The Dog Bay Line: A major Silurian tectonic boundary in northeast Newfoundland. Canadian Journal of Earth Sciences, Volume 30, pages 2481-2494.

Willner, A.P., van Staal, C.R., Zagorevski, A., Glodnye, J., Romere, R.L. and Sudof, M.
2018: Tectonometamorphic evolution along the Iapetus suture zone in Newfoundland: Evidence for polyphase Salinic, Acadian and Neoacadian very low- to medium-grade metamorphism and deformation. Tectonophysics, Volume 742-743, pages 137-167. https://doi.org/10.1016/j.tecto.2018.05.023

Winchester, J.A. and Floyd, P.A.
1977: Geochemical discrimination of different magma series and their differentiation products using immobile elements. Chemical Geology, Volume 20, pages 325-343.

Wood, D.A.
1980: The application of a Th–Hf–Ta diagram to problems of tectonomagmatic classification and to establishing the nature of crustal contamination of basaltic lavas on the British Tertiary Volcanic Province. Earth and Planetary Science Letters, Volume 50, pages 11-30.

Zagorevski, A., van Staal, C.R., McNicoll, V. and Rogers, N.
2007: Tectonic architecture of an arc-arc collision zone, Newfoundland Appalachians. *In* Formation and Applications of the Sedimentary Record in Arc Collision Zones. *Edited by* A. Draut, P.D. Clift and D.W. Scholl. Geological Society of America, Special Paper 436, pages 309-333.